

Large Fractional Bandwidth BAW Filter

M. CHATRAS¹, L. CATHERINOT¹, S. BILA¹, P. BLONDY¹,
D. CROS¹, T. BARON², S. BALLANDRAS²,
P. MONFRAIX³, L. ESTAGERIE⁴

¹University of Limoges, XLIM-CNRS, 123 Av Albert Thomas,
87060 Limoges, France
Tel. : +33 587 50 67 34

²University of Besançon, FEMTO-ST, 32 Av de l'Observatoire,
25044 Besancon, France
Tel. : +33 381 40 28 34

³Thales Alenia Space, 26 Av JF Champollion, 31037 Toulouse, France
Tel. : +33 534 35 60 70

⁴CNES, 18 avenue Edouard Belin, 31 401 Toulouse, France
Tel. : +33 561 28 27 61

Abstract. A resonator using shear waves of lithium niobate is used in this paper to achieve large fractional bandwidth BAW filter. Electromechanical couplings in the 20–50 % range are obtained for the shear waves of a thin layer of Lithium Niobate suspended on a silicon substrate. By this way a filter with fractional bandwidth over 20% has been designed for space applications.

1. Introduction

Acoustic waves in elastic solids are used in numerous applications in signal processing, including frequency generation, control and filtering in modern wireless communication systems [1] [2]. With the growing demand for multimedia and mobile applications, the new generations of telecommunication satellites require higher performances, higher functionalities and still stronger cost and size constraints [3] [4]. In that context, Bulk Acoustic Waves (BAW) devices have many potentialities for the development of smart RF subsystems. For instance this technology is now used as alternative to Surface Acoustic Waves (SAW) filters in handset duplexers for UMTS and DCS standards around 2 GHz with Aluminum Nitride piezoelectric layers [5]. However, Aluminum Nitride is not suitable for large band applications, due to its electromechanical

coupling coefficient. This material is mainly processed for local oscillators or narrowband filtering operations (<5%) [6] [7] [8].

Single crystal-based acoustic resonators for filtering have received a strong interest for many years. Various developments have been particularly achieved using Quartz with either SAW delay lines or resonators. However, most approaches have been developed exploiting quartz machining along standard etching, rarely compatible with batch processes as used for Micro-ElectroMechanical Systems (MEMS) [9][10][11].

That is why Lithium Niobate (LiNbO_3) layers bonded on silicon substrates are studied to reach large band pass specifications for satellite requirements. It is essential to maximize the values of the electromechanical coupling coefficient in Lithium Niobate, and to use wisely crystallographic cuts in order to perform the best results for longitudinal or transverse waves. Thanks to Lithium Niobate shear wave propagation behavior, it is possible to synthesis and to achieve band-pass filters with fractional bandwidth over 10 or 20 %. The resonant frequency of the resonator and the filter proposed in this paper is not given because the industrial partner of this project keeps this value confidential.

2. Electromechanical Coupling Coefficient

Mechanical and electric fields are coupled in piezoelectric solids, so both Maxwell and elastodynamic equations have to be solved [12]. The velocity of elastic waves in elastic solids is generally five orders of magnitude lower than the electric waves, which give much smaller circuits, mainly used for low frequency applications (100MHz ~ 3GHz). A quasi static approximation permits to obtain independent propagations for elastic and electric waves.

By solving the generalized Christoffel equation in piezoelectric materials, we can use tensorial expressions that give phase velocity and polarization [12]. For “z” propagation (fig1.), three plane waves are created, which have orthogonal polarization with different velocities.

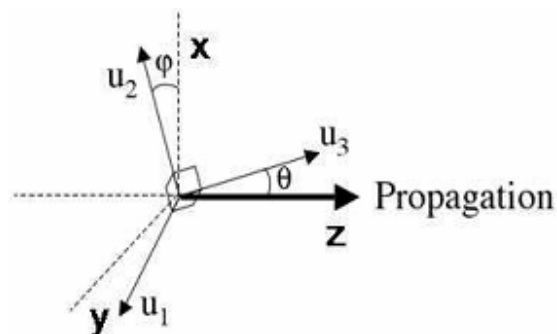


Fig. 1. Propagation in anisotropic crystal.

It results a thickness wave polarized along the “Z” axis, and two shear waves, polarized in the “XY” waves plane. These velocities permit to define very important parameters for BAW resonators: thickness, electromechanical coupling coefficient kt^2 and shear electromechanical coefficient ks^2 .

The higher these coefficients are, the best electromechanical coupling the piezoelectric layer gives. The following expression describes the dependence of kt^2 (or ks^2) according to resonance and anti-resonance.

$$k_t^2 = \frac{\pi^2}{4} \left(\frac{f_p - f_s}{f_p} \right) \quad (1)$$

It is not possible for Aluminum Nitride to have a coupling coefficient kt^2 higher than 7%. We propose to use two different cuts of Lithium Niobate: the (YXl)/36° and the (YXl)/163° cuts. The first one allows for the excitation of high velocity (7000 m.s-1) longitudinal modes whereas shear waves are used in the second one, allowing for electromechanical coupling. For these orientations we obtain ks^2 around 30% for the (YXl)/36° cut and around 45% for the (YXl)/163° cut.

3. 1D Simulation Results

The first step is to size the thicknesses of the several layers of the structure to reach the targeted frequencies. In the case of figure 2, we used the cut Y+36°; we obtain a coupling coefficient kt^2 equal to 33%. This resonator with very large electromechanical coupling will enable to reach easily fractional bandwidth filter over 10%.

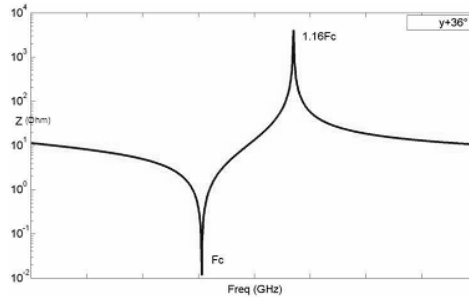


Fig. 2. Simulation response of a lithium niobate resonator (cut Y+36).

4. Fabrication and Measurements

In this work, we propose a filter fabricated on LiNbO₃/Silicon substrates obtained by Au/Au bonding at room temperature and a lapping/polishing on the

upper face of the lithium niobate substrate. This approach allows for a collective and accurate production of filters, the filter frequency being controlled by the membrane thickness of the lithium niobate layer.

We based our device fabrication on gold bonding with a lapping/polishing process to prepare wafer compound to different devices. It allows us to manufacture a BAW resonator on LiNbO_3 membrane as shown in fig. 3. A gold thin layer (200nm) is deposited first by sputtering on both LiNbO_3 (bottom face) and silicon (top face) wafers.

Both wafers are then bonded together via gold layer compression into an EVG bonding machine. During this process, we apply a pressure of 65 N.cm^{-2} to the whole contact surface, yielding a high quality bond. LiNbO_3 is subsequently thinned by lapping and polishing steps to an overall thickness of several microns. The resonator is finally suspended by etching the back side of the silicon substrate by DRIE. Aluminum electrodes are deposited on the LiNbO_3 upon the cavity to achieve working BAW resonators. A cross section of the resonator is presented figure 3.

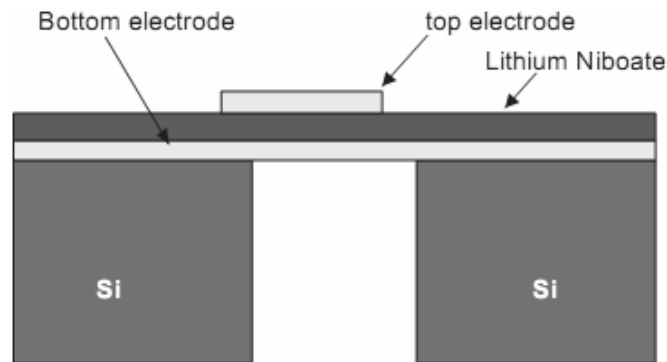


Fig. 3. Cross section of the structure.

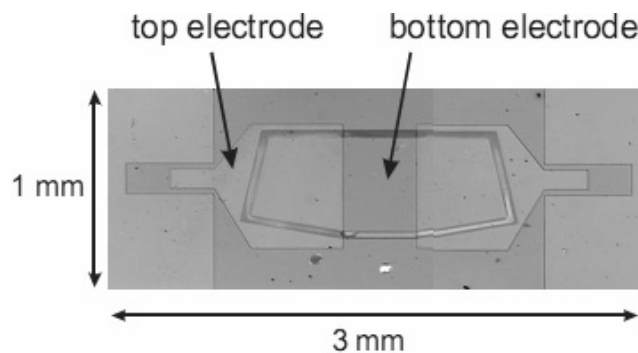


Fig. 4. Fabricated resonator (top view).

S21-parameter measurements for the structure shown in Fig. 4 were performed using a HP 8510 A network analyzer system. The measured response is presented Fig. 5.

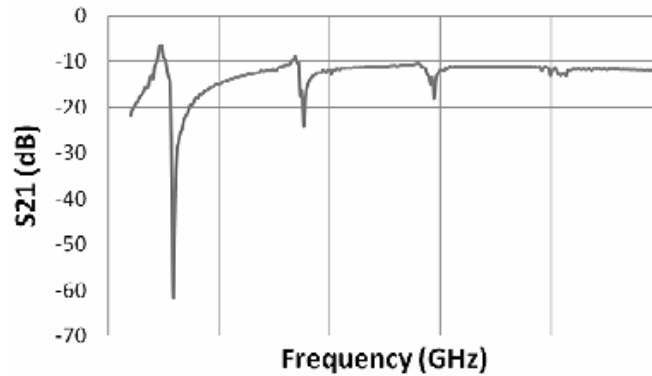


Fig. 5. Measured resonator.

It exhibits an electromechanical coupling of 30 %. This resonator can then be used to synthesis large fractional bandwidth filter. Figure 6 presents a lithium niobate based BAW 3 pole filter with a 3 dB fractional bandwidth of 22 % in a ladder configuration.

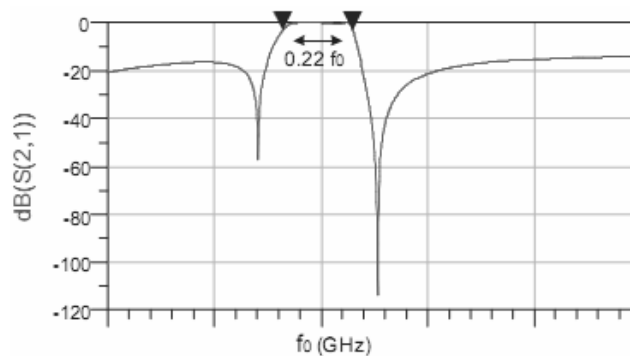


Fig. 6. Computed ladder 3 pole filter with large fractional bandwidth for space application.

5. Conclusion

In this paper an efficient method to compute BAW filter using shear waves has been presented using a scalar approach. By the way very important electromechanical coupling coefficients have been obtained with lithium niobate. Large band pass filter become then very easy to achieve for space applications.

Acknowledgement. This work is supported by the French Space Agency (CNES) (project FOVETTES) under grant# R&T R-S08/TC-0001-026.

References

- [1] K.M. LAKIN, G.R. KLINE, K.T. McCARRON, *High-Q Microwave Acoustic Resonators and Filters*, IEEE Microwave Symp. Digest, **3**, pp. 1517–1520, 1993.
- [2] R. AIGNER, *SAW and BAW Technologies for RF Filter applications: A Review of the Relative Strengths and Weaknesses*, Proceedings of IEEE Ultrasonics Symposium, Beijing/China, 2–5 Nov 2008.
- [3] R. AIGNER, J. KAITILA, J. ELLÄ, L. ELBRECHT, W. NESSLER, M. HANDTMANN, T.-R. HERZOG and S. MARKSTEINER, *Bulk-Acoustic-Wave Filters: Performance Optimization and Volume Manufacturing*, proceedings of IMS-MTTS, Philadelphia, 2003.
- [4] P. BAR, A. GIRY, P. TRIOLET, G. PARAT, D. PACHE, P. ANCEY, J.F. CARPENTIER, *Full duplex receiver and PA integration with BAW devices*, IEEE SiRF, pp. 9–12, 2008.
- [5] S. GIRAUD, S. BILA, M. CHATRAS, D. CROS, M. AUBOURG, *Bulk acoustic Wave Filter Synthesis and Optimization for Multi-Standard communication Terminals*, IEEE TUFFC, **57**, pp. 52–58, January 2010.
- [6] A. REINHARDT, G. PARAT, E. DEFAY, M. AID, F. DOMINGUE, *Acoustic technologies for advanced RF architectures*, IEEE Newcas conference, pp. 161–164, 2010.
- [7] R. LANZ, P. MURALT, *Solidly Mounted BAW Filters for 8 GHz based on AlN Thin Films*, 2003 IEEE Ultrasonic Symp, pp. 178–181.
- [8] C. ZUO, J. van der SPIEGEL, G. PIAZZA, *1.05 GHz CMOS Oscillator based on Lateral-Field-Excited Piezoelectric AlN Contour-Mode MEMS Resonators*, Proc. IEEE Int. Freq. Contr. Symp., pp. 70–74, 2009.
- [9] A. VOLATIER, E. DEFAY, M. AID, A. NHARI, P. ANCEY, B. DUBUS, *Switchable and tunable strontium titanate electrostrictive bulk acoustic wave resonator integrated with a Bragg mirror*, Applied Physics Letters; **92**(3): 032906, 2008.
- [10] G. PIAZZA, P.J. STEPHANOU, A.P. PISANO, *Piezoelectric AluminumNitride Vibrating Contour-Mode MEMS Resonators*, Journal of Microelectromechanical Systems, **15**(6), pp. 1406–1418, Dec. 2006.
- [11] X. ZHU, V. LEE, J. PHILLIPS and A. MORTAZAWI, *Intrinsically switchable contour mode acoustic wave resonators based on barium titanate thin films*, Microwave Symposium Digest, 2009. MTT '09. IEEE MTT-S International, pp. 93–96, 7-12 June 2009.
- [12] K.Y. HASHIMOTO, *RF Bulk Acoustic Wave Filters for Communications*, Artech House, 2009.

An Analogically Tuned Capacitor with RF MEMS Structure

F. BARRIERE, D. MARDIVIRIN, A. POTHIER,
A. CRUNTEANU, P. BLONDY

Xlim Research Institute–UMR 6172 University of Limoges/CNRS 123 avenue
Albert Thomas, 87060 Limoges Cedex, France

Abstract. This paper presents a 102 fF to 18 fF analogically tuned capacitor, based on RF MEMS structure. It is composed of a beam electrostatically actuated with a polarization electrode under, and two RF electrodes above. Then, the operating MEMS principle is inverted, which permits to present a high capacitance variation in the analog motion of the beam, before its pull-down under $2/3$ of the initial gap.

1. Introduction

RF-MEMS are emerging as a practical solution for high Q, wideband tuning of microwave elements. Recently, wide band tunable filters, cavities, and silicon integrated high Q tuners have been demonstrated by several laboratories and companies. Indeed, specific designs had to be made or very careful integration of varactors had to be conducted. Among the designs that have been made in RF-MEMS switched varactors, most were concentrated on high density capacitance designs, which resulted in moderate Qs, when they were switched in the down state. In the design presented in [1] and [2], the capacitance is operating in the opposite manner: the electrostatic gap is in the lower side of the capacitor, and the capacitance is decreased as the voltage is increased. Therefore, instability issues are occurring when the moveable plate is far from the actuation plate. Another approach could be to use a structure similar to ohmic contact switches with a capacitive contact instead of having an ohmic contact. This idea was developed in [3] and [4]. In this paper, we propose to develop novel air gap capacitance, with low values and high Q, and a normally on behavior, that is to say the device has its largest capacitance when no bias voltage is applied. A photograph of the RF MEMS varactor is presented in Fig. 1.

2. Operating and Fabrication

The varactor presented is based on an RF MEMS technology developed already, and presented in [5]. It is composed of an electroplated gold bridge raised above an actuation electrode made in chromium, and an aluminum nitride dielectric layer. The microwave input and output are standing above the bridge, with an air gap between both. The varactor corresponds to two capacitance in series located at the RF input of the bridge (metal-air-metal capacitance), and the same with the output. These two capacitances will decrease by applying bias, which reduces the bridge height, and increases the distance with microwave input and output.

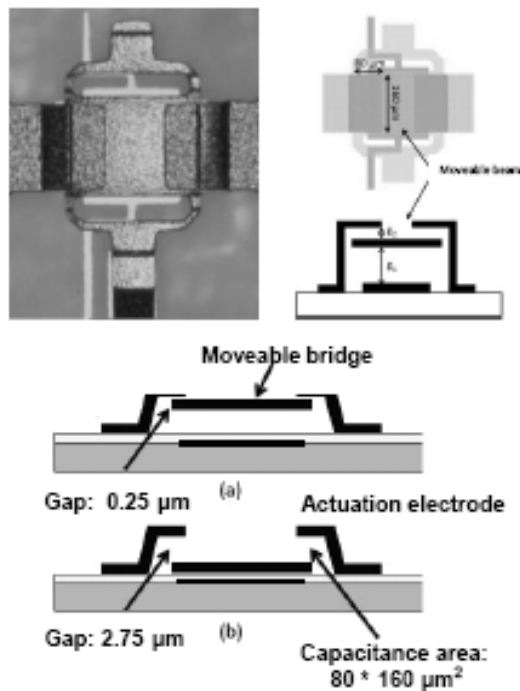


Fig. 1. Photograph of the micrometric RF MEMS varactor, and its operating sketch view under.

In order to reduce losses in the structure, the bridge and RF electrodes thickness are $3 \mu\text{m}$ thick. Thus, the series resistance due to metallization is strongly decreased, and the Q factor of the capacitance is less limited by this parameter. The bridge is raised upon the dielectric layer with a $2.50 \mu\text{m}$ height, leaving a variable distance from $0.25 \mu\text{m}$ to $2.75 \mu\text{m}$ with the RF electrodes. The AlN dielectric layer thickness is 400 nm . The fabrication process of this component is shown in Fig. 2.

This design of RF-MEMS allows a variation of capacitance in the 5 V to 30 V range.

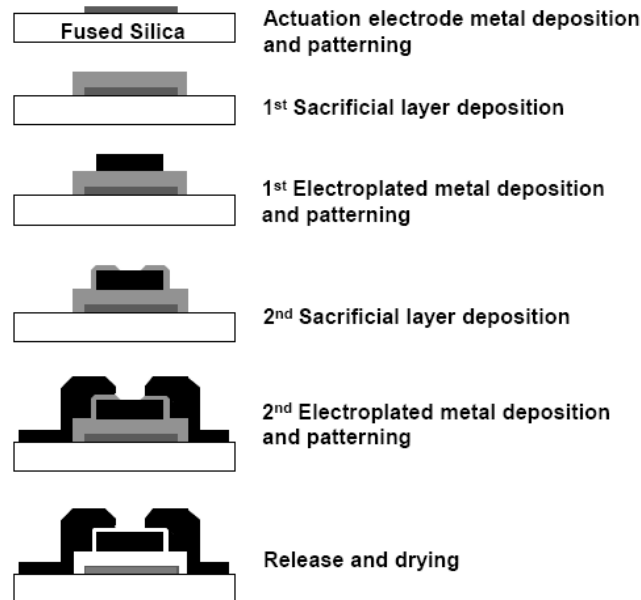


Fig. 2. Fabrication process of the RF MEMS based varactor.

3. Measurements

Measurements were taken on an Agilent-HP 8722 ES VNA, and cascade probe stations, as the component has been implemented on a coplanar waveguide. The values of the capacitors were fitted to an equivalent scheme composed of capacitance in series with a 0.29 nH inductance. The capacitance values were fitted to the measured curves, with relatively fair agreement. The measured up state capacitance is 102 fF, and the down state capacitance is 12 fF, with the beam contact on the dielectric. The lowest capacitance measured in the analog range is 18 fF, with 35 V applied in the electrostatic actuator. Measurements are shown in Fig. 3., where we try to pick-up the varactor capacitance value each 0.5 dB of variation. On these curves the highest capacitance corresponds to the beam initial state, with no bias applied. Finally, this device presents analog capacitance variation with a ratio of 5.6, and a switched capacitance variation with 8.5.

Regarding loss, we were not able to measure any consistent value for the Q of these varactors. The modulus of the impedance of the series capacitance is over 1 KOhm at 2 GHz, even in the up state, and we estimate that the series resistance of this device is on the order of 0.1 Ohm.

We believe that the main loss contribution of such varactor mounted inside a microwave cavity will be the assembly loss. For instance, if the bonding resistance is Ohm, then the Q of this device would be better than 100 at 10 GHz, in the worst case, since the capacitance is low.

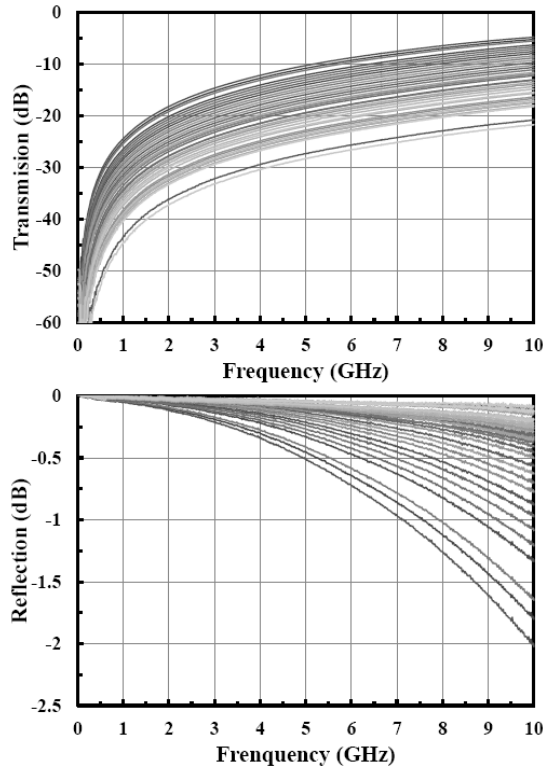


Fig. 3. RF measurements of the varactor under various bias, from 0 V applied ($C = 102$ fF) to 36 V ($C = 12$ fF). The lowest capacitance value in the analog part is obtain at 35 V with $C = 18$ fF.

4. RF-Power

On this type of structure, the RF electrodes are opposed to the actuator electrode, compared to the moveable beam. This is an important point, because the effect of RF power will applied on the beam a force opposed to the electrostatic force. Thus, failure modes like self-actuation can be compensate by applying an appropriate added voltage on the actuator. The Fig. 4. shows the effect of power on the varactor during a power sweep from 10 mW to 1 W for different initial capacitance values, and the power compensation with biasing. All RF power are applied at frequency constant wave of 3 GHz.

We can see first that the power effect increases the varactor’s capacitance value, especially when the beam is near RF electrodes. The failure by contact between the beam and RF electrodes is identified at 26 dBm applied for capacitance values of almost 100 fF. This failure happens with higher RF power when the capacitance is lower, as the beam goes away from RF electrodes, until no

influence observed at the analog limit ($S_{21}=-26$ dB @ 3 GHz), and after pull-down.

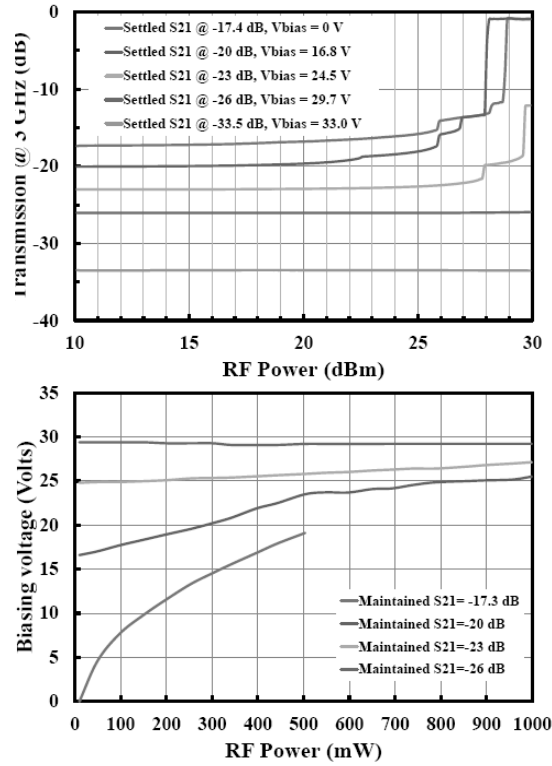


Fig. 4. On the top: effect of RF power on the varactor with fixed biasing voltages, the capacitance increase with power until failure. On the bottom: compensated RF power effect with biasing to fix the capacitance values.

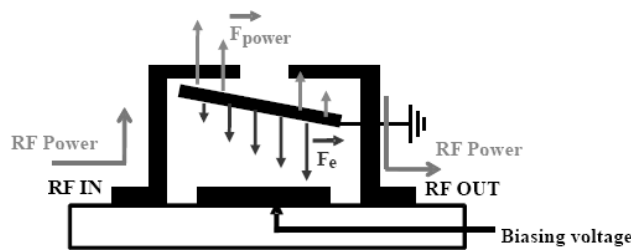


Fig. 5. The RF power effect compensation is limited, considering that the force induced by power is non-uniformly distributed on the moveable beam.

The power effect is compensated by applying higher bias voltage, so higher electrostatic force, which permits to equilibrate the beam height at a given position

(also the RF transmitted response). At the initial state, the beam is near the RF electrode with no bias applied. When RF power increases, bias voltage is applied on the actuator to compensate. We can see that almost 20 V are needed to compensate 500 mW of power. After this step, the compensation cannot be established, because the mechanical force induced by power is not uniformly distributed on the beam, so the beam will be positioned slantwise, and failure by contact between beam and RF-electrode cannot be prevented (Fig. 5.).

For lower capacitance values, the beam is located lower, and the power effect can be compensated until 1 W.

5. Conclusion

We have presented an analogically tuned RF MEMS varactor, based on a reverse actuation principle. This type of structure shows the potential to design microwave devices with very high quality factor and enough wide accordability. Furthermore, high quality factor are developed on very low value of variable capacitances (<100 fF).

Capacitance range of this type of device can be easily changed in the conception, because it is almost only dependent of RF electrodes surfaces, considering that the mechanical part of the structure is not sensitive to this parameter.

Finally, another point can be interesting, considering that the biasing electrode can be used to compensate the effect of RF power, and then permit to increase the reliability of the device with high power handling.

Acknowledgment. Authors want to acknowledge the French Ministry of Defense for their support in this work.

References

- [1] Xiaoguang LIU, Linda P.B. KATEHI, William J. CHAPPELL and Dimitrios PEROULIS, *A 3.4 - 6.2 GHz Continuously Tunable Electrostatic MEMS Resonator with Quality Factor of 460-530*, IEEE MTT-S Int. Microwave Symp. Dig., June 2009.
- [2] J. HIMANSHU, H.H. SIGMARSSON, P. DIMITRIOS and W.J. CHAPPELL, *Highly loaded evanescent cavities for widely tunable high-Q filters*, IEEE MTT-S Int. Microwave Symp. Dig., pp. 2133–2136, June 2007.
- [3] Alex GRICHENER, Balaji LAKSHMINARAYANAN and Gabriel M. REBEIZ, *High-Q RF MEMS Capacitor with Digital/Analog Tuning Capabilities*, IEEE MTT-S Int. Microwave Symp. Dig., June 2008.
- [4] S. FOULADI, W. DONG YAN and R.R. MANSOUR, *Microwave Tunable Bandpass Filter with MEMS Thermal Actuators*, Proceedings of the 38th European Microwave Conference.
- [5] F. BARRIERE, A. CRUNTEANU, A. POTHIER, M. CHATRAS, P. BLONDY, *A Low Value Normally On RF-MEMS Switches Capacitor For High Q Millimeter Wave Tuning*, IEEE SiRF Conference., pp. 77–79, Jan. 2010.